A novel bifunctional aldehyde/alcohol dehydrogenase mediating ethanol formation from acetyl-CoA in hyperthermophiles

Qiang Wang
Jiangsu University
Chong Sha
Jiangsu University
Hongcheng Wang
Jiangsu University
Kesen Ma
University of Waterloo
Juergen Wiegel
University of Georgia
Abd El-Fatah Abomohra
Tanta University
Weilan Shao (weilanshao@foxmail.com)
Jiangsu University

Research

Keywords: Acetyl-CoA reduction, Bifunctional aldehyde/alcohol dehydrogenase, Ethanol fermentation, Hyperthermophiles, Thermotoga neapolitana

Posted Date: March 15th, 2020

DOI: https://doi.org/10.21203/rs.3.rs-17223/v1

Abstract

Background: Hyperthermophilic fermentation at temperatures above 80 °C allows *in situ* product removal to mitigate the ethanol toxicity, and reduces microbial contamination without autoclaving/cooling of feedstock. Many species of *Thermotoga* grow at temperatures up to 90 °C, and have enzymes to degrade and utilize lignocelluloses, which provide advantages for achieving consolidated processes of cellulosic ethanol production. However, no CoA-dependent aldehyde dehydrogenase (CoA-Aldh) from any hyperthermophiles has been documented in literature so far. The pyruvate ferredoxin oxidoreductases from hyperthermophiles have pyruvate decarboxylase activity, which convert about 2% and 98% of pyruvate to acetaldehyde and acetyl-CoA (ac-CoA), respectively. Acetyl-CoA can be converted to acetic acid, if there is no CoA-Aldh to convert ac-CoA to acetaldehyde and further to ethanol. Therefore, the current study aimed to identify and characterize a CoA-Aldh activity that mediates ethanol fermentation in hyperthermophiles.

Results: In *Thermotoga neapolitana* (*Tne*), a hyperthermophilic iron-acetaldehyde/alcohol dehydrogenase (Fe-AAdh) was, for the first time, revealed to catalyze the ac-CoA reduction to form ethanol via an acetaldehyde intermediate, while the annotated *aldh* gene in *Tne* genome only encodes a CoA-independent Aldh that oxidizes aldehyde to acetic acid. Three other *Tne* alcohol dehydrogenases (Adh) exhibited specific physiological roles in ethanol formation and consumption: Fe-Adh2 mainly catalyzed the reduction of acetaldehyde to produce ethanol, and Fe-Adh1 showed significant activities only under extreme conditions, while Zn-Adh showed special activity in ethanol oxidation. In the *in vitro* formation of ethanol from ac-CoA, a strong synergy was observed between Fe-Adh1 and Fe-AAdh. The Fe-AAdh gene is highly conserved in *Thermotoga* spp. and in *Pyrococus* sp., which is probably responsible for ethanol metabolism in hyperthermophiles.

Conclusions: Hyperthermophilic *Thermotoga* spp. are excellent candidates for biosynthesis of cellulosic ethanol fermentation strains. The finding of a novel hyperthermophilic CoA-Aldh activity of *Tne* Fe-AAdh revealed the existence of a hyperthermophilic fermentation pathway from ac-CoA to ethanol, which offers a basic frame for *in vitro* synthesis of a highly active AAdh for effective ethanol fermentation pathway in hyperthermophiles, which is a key element for the approach to the consolidated processes of cellulosic ethanol production.

Background

As a leading candidate among alternatives to petroleum-derived transportation fuels, the production of fuel ethanol from cellulosic biomass has received considerable attention and effort over the last two decades [1, 2]. However, the high costs of converting biomass to sugars and distilling ethanol at low concentrations from fermentation products are the primary factors that impede the establishment of a cellulosic biofuels industry [1, 3]. Thermophiles can produce cellulosic ethanol at a high temperature, where ethanol is directly distillated from fermentation, and biodegradation of lignocellulose can be simultaneously achieved when these thermophiles carry and express cellulase and hemicellulase genes [3, 4]. Metabolic engineering of microorganisms has been an effective approach to improve the strains of cellulosic ethanologenic thermophiles.

Thermophiles can be categorized into three groups based on their optimal growth temperatures: Moderate thermophiles grow optimally between 50–64 °C; extreme thermophiles and hyperthermophiles can grow optimally between 65–79 °C and above 80 °C, respectively [5, 6]. Extreme thermophiles such as Thermoanaerobacter ethanolicus (Tet) and Thermoanaerobactrium spp. that have been successfully modified by pathway modification for producing ethanol at elevated yields [1, 7], can grow optimally up to 69 °C with xylan as a substrate. Metabolic engineering of cellulolytic thermophiles for ethanol production can reduce the costs for the pretreatment of biomass and the addition of exogenous cellulase. Caldicellulosiruptor bescii is a cellulolytic thermophile that grows optimally at 72–75 °C [8]. A lactate dehydrogenase (Ldh) deletion mutant of C. bescii was engineered to produce up to 2.3 mM ethanol on Avicel at 75 °C by cloning and expressing aldehyde/alcohol dehydrogenase (AAdh) genes from Tet [9]. Furthermore, thermophilic fermentation at temperatures above the boiling point of ethanol could allow in situ product removal to mitigate ethanol toxicity. Basen et al. [10] aimed to modify a hyperthermophilic archaeon by inserting an alcohol dehydrogenase (Adh) gene into the genome of Pyrococcus furiosus (Pfu) to drive bioalcohol production.

Thermotoga spp. are cellulolytic and hemicellulolytic hyperthermophiles that meet the requirements for the construction of a cellulosic ethanol producer. However, the genes encoding hyperthermophilic enzymes for an effective ethanol metabolic pathway should be able to function in the organisms grown at temperatures above 80 °C. The final steps of ethanol fermentation in anaerobes are two reversible redox reactions, from acetyl-CoA (ac-CoA) to acetaldehyde (ac-ald) catalyzed by the CoA-dependent aldehyde dehydrogenase (Aldh) (enzyme classification number, EC 1.2.1.10), and from ac-ald to ethanol catalyzed by Adh. Researchers have been focusing their efforts on Aldh and Adh since 1988 [11, 12]. Nevertheless, a CoA-dependent Aldh has not yet been identified in any of the hyperthermophilic strains, although there are CoA-independent Aldhs (EC 1.2.1.3) catalyzing the irreversible oxidation of the aldehydes to their corresponding acids [13].

The aim of this study was to determine the properties of putative Adhs in Thermotoga species. In particular, the way in which they function under imitative physiological conditions was studied to reveal their possible roles in ethanol formation and consumption. T. neapolitana (Tne) grows at temperatures up to 90 °C [14], and has genes coding for a series of enzymes for lignocellulose degradation and utilization (GenBank accession No. CP000916.1). In this paper, we report the heterogeneous expression and purification of Aldh and Adhs from Tne, and the biochemical and physiological properties of the recombinant enzymes. In addition, the in vitro ethanol production catalyzed by Fe-AAdh was examined in the

presence of one of the other Adhs. In addition, the plausibility of using metabolically engineered Thermotoga spp. as a means to produce ethanol at temperatures of approximately 80 °C from cellulosic biomass was discussed.

Results

Gene cloning, expression, and enzyme purification

To prepare recombinant enzymes encoded by Tne genes CTN_0257, CNT_0580, CTN_1548, CTN_1655 and CTN_1756, these genes were amplified from Tne genomic DNA, and successfully cloned into E. coli expression vector pHsh to generate plasmids pHsh-0257, pHsh-0580, pHsh-1548, pHsh-1655, and pHsh-1756. The target genes in the expression plasmids were sequenced and it was confirmed that no mutation had occurred in them. All the expression plasmids were transformed into E. coli and the target genes were successfully induced to express in the recombinant cells (Fig. 1).

The recombinant proteins produced from Tne genes CTN_0257, CNT_0580, CTN_1548, CTN_1655, and CTN_1756 were designated as Zn-Adh, Fe-AAdh, Aldh, Fe-Adh1, and Fe-Adh2, based on their activities and metal ions, and the gene products had subunits similar to their putative molecular masses of 43.3, 42.6, 51.8, 40.6 and 43.6 kD, respectively (Fig. 1). These enzymes were purified to near gel electrophoresis homogeneity after heat treatment and metal affinity chromatography using Ni-column at room temperature (Fig. 1). However, the purified Fe-AAdh, Fe-Adh1, and Fe-Adh2 became inactivated within about a week after they were stored at -20 °C, implying that they were sensitive to O_2 in the air and buffer. This problem was resolved by purifying these enzymes in an anaerobic chamber using degassed buffers and keeping the purified enzyme in sealed anaerobic serum tubes.

Intracellular conditions in the growing Tne cells

Biochemical characterization of these enzymes can reveal properties and potentials of each enzyme. However, the conditions in a living cell are equilibrated for a sustainable life, and most intracellular conditions do not meet the optimal reaction conditions of an enzyme. It is important to estimate how the enzymes catalyze energy metabolisms under physiological conditions in cells growing at about 80 °C and pH 7.0 or lower, where the reduced and oxidized forms of cofactors are present at the same time to support both the forward and reverse reactions in the cytoplasm.

The pH value and cofactor concentrations of NAD^+, NADH, $NADP^+$, and NADPH are usually limited to certain levels. Under chemostatic conditions, NAD^+, NADH, $NADP^+$, and NADPH concentrations determined for Clostridium acetobutylicum cells were 6.8, 0.97, 0.41, and < 0.2 μmol/g of dry cells, which are 1.30, 0.19, 0.08, and 0.04 μmol/g of wet cells, respectively [12, 15]. In this work, the pH value of nonbuffered Tne cell extracts was 6.5, which is might be approximately the intracellular pH of the cells in middle exponential phase of growth. The intracellular concentrations of NAD^+, NADH, $NADP^+$, and NADPH were determined as 1.8, 0.28, 0.18, and 0.06 mM in Tne cells in late logarithmic phase (Fig. 2a).

The concentration of substrates is an important parameter affecting enzyme activity. However, currently no method is known for determining the intracellular concentrations of the substrates, such as ac-CoA and ac-ald, for the final steps of ethanol fermentation pathway. Instead, we determined the tolerance of Tne cells to ac-ald and ethanol, which might indicate how much of those substances would inhibit cell growth. The tests revealed that the growth rate of Tne cells was reduced by 50% in the presence of about 1.7 mM ac-ald, while 120 mM ethanol in the medium reduced growth rate by about 25% (Fig. 2b). These results indicate that Tne can tolerate certain amount of ethanol, but it is very sensitive to ac-ald, which must be transiently reduced or oxidized in living cells.

Biochemical properties of the recombinant enzymes

Four possible reactions can occur in the final steps of ethanol formation from acetyl-CoA. To determine the number of steps each dehydrogenase can catalyze, the biochemical properties of the enzymes were characterized at their optimal reaction pH and temperatures, where substrate(s) and cofactor concentrations were approximately 10 times higher than the K_m value of the enzyme. Among the five recombinant enzymes, Tne Aldh encoded by gene CTN_1548 catalyzed the oxidation of various aldehydes using either NAD^+ or $NADP^+$ as coenzyme, while it did not show any ac-CoA reduction activity. The main biochemical properties of recombinant enzymes encoded by Tne genes CTN_0257, CNT_0580, CTN_1655 and CTN_1756 are listed in Table 1.

Table 1

Optimal reaction conditions and cofactor dependences for the enzymes of hyperthermophilic ethanol fermentation pathway.

Enzyme (gene)	**Fe-AAdh (CNT_0580)**				**Fe-Adh1 (CTN_1655)**		**Fe-Adh2 (CTN_1756)**		**Zn-Adh (CTN_0257)**	
Reaction	Ac-CoA→Ac-ald	Ac-CoA←Ac-ald	Ac-ald→Eth	Ac-ald←Eth	Ac-ald→Eth	Ac-ald←Eth	Ac-ald→Eth	Ac-ald←Eth	Ac-ald→Eth	Ald←Eth
pH_{opt}	7.0	9.0	7.0	8.5	8.5	8.5	7.0	8.5	-	5.8
T_{opt}	85℃	85℃	80℃	95℃	95℃	95℃	85℃	100℃	-	95℃
Spec activity										
NADPH	0.92 ± 0.03		3.27 ± 0.05		0.70 ± 0.05		3.09 ± 0.06		ND	
NADH	ND		0.52 ± 0.06		ND		ND		ND	
NADP		0.41 ± 0.01		2.44 ± 0.04		0.43 ± 0.05		1.20 ± 0.06		0.46 ± 0.03
NAD		0.16 ± 0.02		0.36 ± 0.05		0.22 ± 0.04		0.25 ± 0.04		0.30 ± 0.02

Ac-CoA, acetyle-CoA; Ac-ald, acetaldehyde; Eth, ethanol; ND, activity not detectable.

Table 1 Optimal reaction conditions and cofactor dependences for the enzymes of hyperthermophilic ethanol fermentation pathway. (Attached file)

When searching for an enzyme that could reduce ac-CoA to ac-ald, we found that purified enzyme encoded by CNT_0580 was a bifunctional aldehyde/alcohol dehydrogenase (Fe-AAdh) that could catalyze all the forward and reverse reactions in the pathway from ac-CoA to ethanol under optimal reaction conditions (Table 1). Fe-AAdh catalyzed forward reactions from Ac-CoA to ethanol optimally at pH 7.0 and the reverse reactions at pH 8.5 or higher (Fig. 3a). Fe-Adh1 and Fe-Adh2 catalyzed the forward and reverse reactions between ac-ald and ethanol without showing any ac-CoA reduction activity. However, the activity of Fe-Adh1 was much lower than that of Fe-Adh2. In comparison, Fe-Adh1 not only had lower activities, but also had higher pH and temperature optima than Fe-AAdh and Fe-Adh2 (Table 2). Therefore, Fe-Adh2 and Fe-AAdh were the main reactive enzymes for ethanol formation at the pH range that was approximately the intracellular pH of the middle exponential phase of cell growth (Fig. 3b). The Tne Zn-Adh specifically catalyzed the reaction from ethanol to ac-ald, and no activity was detected for the reaction from ac-ald to ethanol. This result is different from almost all the other Adhs reported previously [11, 12, 16]. The activities of these enzymes depended highly on the pH conditions of the reaction mixtures. Tne Zn-Adh reacted optimally at pH 5.8, which was close to pH 6.5, the pH value of non-buffered cell-free extracts of Tne. The CoA-independent Aldh had an optimal pH of 9.5, which together with Zn-Adh could form a detoxification system for the oxidation of ethanol and aldehyde.

Table 2
Kinetics of the enzymes under imitative physiological conditions at 80 °C and pH 6.5.

Enzyme (gene)	Fe-AAdh (CTN_0580)				Fe-Adh1 (CTN_1655)		Fe-Adh2 (CTN_1756)		Zn-Adh (CTN_0257)	
Reaction	Reduction	Oxidation	Reduction	Oxidation	Reduction	Oxidation	Reduction	Oxidation	Reduction	Oxidation
Reaction	Ac-CoA→Ac-ald	Ac-CoA←Ac-ald	Ac-ald→Eth	Ac-ald←Eth	Ac-ald→Eth	Ac-ald←Eth	Ac-ald→Eth	Ac-ald←Eth	Ac-ald→Eth	Ac-ald←Eth
Co-factor(s) [a]	NADPH [b]	Mixture	Mixture	Mixture	Mixture	Mixture	Mixture	Mixture	Mixture	
Substrate	Ac-CoA	Ac-ald + CoA	Ac-ald [b]	Eth	Ac-ald	Eth	Ac-ald [b]	Eth	Ac-ald	Eth [b]
K_m (mM)	0.23 ± 0.02	ND	1.24 ± 0.03	ND	ND	ND	2.75 ± 0.06	ND	ND	80.7 ± 1.68
V_{max} (U/mg)	0.26 ± 0.01	ND	2.49 ± 0.22	ND	ND	ND	2.79 ± 0.04	ND	ND	0.58 ± 0.01

Ac-CoA, acetyle-CoA; Ac-ald, acetaldehyde; Eth, ethanol; ND, activity not detectable.

[a] Cofactor mixture, 1.8 mM NAD, 0.28 mM NADH, 0.18 mM NADP, and 0.06 mM NADPH.

[b] These substrates were used in various concentrations for determining K_m and V_{max} values.

Properties of Fe-AAdh in catalyzing ac-CoA reduction

Fe-AAdh was the first enzyme found in hyperthermophiles that catalyzed the reduction of ac-CoA to produce ac-ald. In addition to its reaction optima (Table 1), this enzyme was subjected to further characterization. Fe-AAdh had 1-h half-life at about 92 °C, which is a typical property of hyperthermophilic enzymes (Fig. 3c). When analyzed at 85 °C and pH 6.5, the activity of Fe-AAdh to catalyze ac-CoA reduction strongly depended on the concentration of NADPH. Although its specific activity was upto 0.92 at pH 7.0 (Table 1), the apparent K_m and V_{max} were 0.23 mM NADPH and 0.26 U/mg at pH 6.5 in the absence of NADH and NAD(P)$^+$, and there was significant substrate inhibition when NADPH concentration exceeded 0.4 mM (Fig. 3d). At the imitated physiological concentrations of cytoplasm for the mixture of NAD(P)H and NAD(P)$^+$, Fe-AAdh did not show activity in catalyzing ac-CoA reduction. It could be because 0.06 mM NADPH was a low concentration in the cells, which was detected after the reducing power had been dumped via H_2 formation. Furthermore, the presence of NADH, NAD$^+$, or NADP$^+$ affected ac-CoA reduction activity by Fe-AAdh; the activity was increased by NADH and inhibited by NAD$^+$ and NADP$^+$ at physiological concentrations (Fig. 3e). The presence of the complex of 0.28 mM NADH, 1.8 mM NAD$^+$, and 0.18 mM NADP$^+$ resulted in a net decrease of V_{max} (0.17 U/mg) along with an increase of K_m (0.55 mM) (Fig. 3d).

Conversion of ac-ald to ethanol under imitative physiological conditions

To estimate the physiological roles of Fe-AAdh, Fe-Adh1, Fe-Adh2, and Zn-Adh in growing cells, enzyme activities were evaluated under physiological conditions similar to those in cytoplasm, which contained mixed cofactors (1.8 mM NAD$^+$, 0.28 mM NADH, 0.18 mM NADP$^+$, and 0.06 mM NADPH), pH 6.5, with 2 mM ac-CoA, ac-ald, or CoASH. In biochemical characterization under optimized conditions, Fe-AAdh, Fe-Adh1 and Fe-Adh2 exhibited significant activities in both ac-ald reduction (forward) and ethanol oxidation (reverse) reactions. However, under the imitative physiological conditions, all these three enzymes did not have significant activity to catalyze the reverse reaction between ac-ald and ethanol (Table 2). Therefore, Zn-Adh was the enzyme only able to catalyze the reduction of ethanol to ac-ald with a K_m of 80 mM ethanol under imitative physiological conditions (Table 3), indicating that the physiological role of this enzyme is likely the catalysis of detoxification reaction when ethanol concentration is high.

Table 2 Kinetics of the enzymes under imitative physiological conditions at 80 °C, pH 6.5. (Attached file)

For the forward reaction of ac-ald to ethanol, Fe-Adh1 did not have any detectable activity under imitative physiological conditions, probably because its activity was weak and its optimal reaction pH is much higher than the pH value detected in non-buffered cell-free extract. Therefore, Fe-AAdh and Fe-Adh2 are the main enzymes catalyzing the reduction of ac-ald. They might contribute equally to ethanol formation because they showed similar V_{max}. However, Fe-AAdh showed a lower K_m values for its substrate ac-ald compared to that of Fe-Adh2 (Table 2). Thus Fig. 3f summarizes the main roles of these enzymes in ethanol metabolic pathway as revealed through the present study.

In vitro ethanol formation

To confirm their physiological roles, Fe-AAdh, Fe-Adh1, Fe-Adh2, and Zn-Adh were used for in vitro formation of ethanol from ac-CoA. In the tests using ac-CoA and NADPH as substrates, ethanol was detected at new peaks in HPLC and GC profiles after Fe-AAdh catalysis (Fig. 4). The effects of alcohol dehydrogenases on ethanol formation were determined by adding Fe-Adh1, Fe-Adh2, or Zn-Adh into the reaction mixture of Fe-AAdh. Interestingly, all the three alcohol dehydrogenases, including Zn-Adh that showed activity only for ethanol oxidation, enhanced ethanol formation from ac-CoA (Fig. 4). The addition of 19 μg Fe-Adh2 into the reaction mixture of 47 μg Fe-AAdh resulted in 9.5 times increase of ethanol formation from ac-CoA, where ac-CoA reduction was catalyzed by Fe-AAdh alone and ac-ald reduction could be catalyzed by both Fe-AAdh and Fe-Adh2 (Table 3). These results reveal the complicate interactions of these enzymes in a biological system, and there is a strong synergy between the aldehyde and alcohol dehydrogenase activities. To explain why Zn-Adh, an enzyme did not show any acetaldehyde reduction activity, could have any stimulation of the ethanol formation, and how Fe-Adh2 stimulate ethanol production by 9.5 times, new methods are required for a further research.

Table 3
In vitro catalysis of ethanol formation from acetyl-CoA

Enzyme(s)	Fe-AAdh	Fe-AAdh + Fe-Adh1	Fe-AAdh + Fe-Adh2	Fe-AAdh + Zn-Adh
Peak area	1074 ± 126	1147 ± 180	5507 ± 236	4604 ± 356
Ethanol titer (mM)	0.081 ± 0.020	0.092 ± 0.028	0.773 ± 0.037	0.633 ± 0.056
Relative activity (%)	100	113	954	781
Reaction mixture (100 μl) contains 5 mM acetyl-CoA, 5 mM NADPH, 100 mM MOPS at pH 7.5, and 47 μg Fe-AAdh with or without addition of Fe-Adh1 (22 μg), Fe-Adh2 (19 μg), or Zn-Adh (43 μg).				

Bioinformatics of Fe-AAdh protein

The amino acid sequence of Fe-AAdh was subjected to the multiple sequence alignment (MSA) using the program T-Coffee and ESPript (Easy Sequencing in PostScript, http://espript.ibcp.fr/ESPript/ESPript/index.php) [17, 18]. The results revealed that the same enzyme appeared in hyperthermophilic Thermotoga spp. and archaea species (Table 4), which is annotated as iron-containing alcohol dehydrogenase (ADH). The amino acid sequences were also compared between Fe-AAdh and the other bifunctional aldehyde/alcohol dehydrogenases, AdhB an AdhE (Fig. 5). Interestingly, AdhE is a large protein with two domains of Fe-ADH (PF00465 family) and an ALDH (ALDH-SF superfamily) while bifunctional enzymes of Fe-AAdh and AdhB are similar to a monofunctional ADH such as Fe-Adh2 (Fig. 5). Meanwhile, Fe-AAdh and AdhB belong to the iron- and zinc-containing alcohol dehydrogenase families, respectively. These results indicate that these enzymes employ different strategies to achieve CoA-dependent aldehyde dehydrogenase activities.

Table 4
Distribution of Fe-AAdh in hyperthermophiles

Microorganism	GenBank accessory No.	Pfam family	Sequence similarity
Thermotoga neapolitana DSM 4359	CTN_0580	PF00465 (Fe-ADH)	100%
Thermotoga maritima MSB8	TM_0111	PF00465 (Fe-ADH)	100%
Thermotoga sp. RQ7	TRQ7_04415	PF00465 (Fe-ADH)	100%
Thermotoga petrophila	Tpet_0813	PF00465 (Fe-ADH)	99%
Pyrococcus furiosus DSM 3638	PF_0075	PF00465 (Fe-ADH)	94%
Thermococcus kodakarensis (ATCC BAA-918)	TK_RS07830	PF00465 (Fe-ADH)	93%

Discussion

Metabolic engineering has proven to be an effective approach to construct novel ethanol-producing strains by heterogeneous expression of the genes coding for the enzymes catalyzing reactions involved in ethanol formation [9, 10]. At present, research has been focused on the identification of hyperthermophilic enzymes involved in the ethanol fermentation pathway. The pyruvate ferredoxin oxidoreductases (POR or PFOR) from T. maritima (Tma) and T. hypogea (Thy) were found to have CoA-dependent pyruvate decarboxylase (PDC) activity, where the PDC activity is less than 2% of POR activity [19, 20]. Thus, more than 98% of pyruvate is probably converted to ac-CoA by POR, and ac-CoA is further converted to acetic acid if there is no enzyme to catalyze the reduction of ac-CoA to produce ac-ald (Fig. 6a). Therefore, the present work focused on searching and improving a hyperthermophilic enzyme that catalyzes the reduction of ac-CoA for a more effective ethanol fermentation pathway (Fig. 6b). Previous studies on the ethanol fermentation pathway of anaerobic thermophiles found that the CoA-dependent Aldh activity is performed by the enzymes annotated as alcohol dehydrogenases such as AdhB and AdhE [21, 22]. There is a gene in Tne genome annotated as

Aldh, but it was confirmed in this work that the gene product was a CoA-independent Aldh. Therefore, it is necessary to identify the physiological roles of the enzymes encoded by the ADH genes in hyperthermophilic species of Thermotoga. This paper reports the study on the four genes annotated as iron or zinc containing ADH genes; only two genes not included in this study are those annotated as alcohol dehydrogenase GroES domain protein (CTN_0385, & CTN_0369) in Tne genomic sequence.

A typical thermophilic anaerobic ethanol metabolism pathway is found in Tet, an extreme thermophile that produces ethanol as the main product via the activities of AdhA, AdhB, and AdhE [12, 23]. Genomic sequence analysis showed no genes encoding protein similar to AdhB or AdhE in hyperthermophilic species of Thermotoga. Our results confirm that the enzyme system of the ethanol metabolism pathway in hyperthermophiles differs from that in extreme thermophiles. Under imitative physiological conditions, the AdhA, AdhB, and AdhE are able to reversibly catalyze the reduction and oxidation reactions [12]; however, Fe-AAdh and Fe-Adh2 activities with respect to the oxidation of ac-ald and ethanol were too low to be detectable because cytoplasmic pH is lower than their pH_{opt}. The presence of the reduced form of cofactors may also hinder the reverse reaction by supporting forward reaction (Table 2). Therefore, each enzyme in hyperthermophilic system catalyzes a reduction or oxidation reaction specifically, rarely both (Fig. 3f).

Bifunctional aldehyde/alcohol dehydrogenases are essential for ethanol metabolism after pyruvate:ferredoxin oxidoreductase catalyzes coenzyme A and oxidative decarboxylation of pyruvate to ac-CoA [12, 24]. As a biofunctional aldehyde/alcohol dehydrogenase, Fe-AAdh of Tne displayed properties different from those of AdhB and AdhE of Tet under imitative physiological conditions. Both AdhB and AdhE have very weak ac-ald reduction activities while AdhE has very high ac-CoA reduction activity, and therefore, the rate limiting step for ethanol formation is the ac-ald reduction in Tet. In Tne, however, Fe-AAdh and Fe-Adh2 exhibited high ac-ald reduction activity, and only Fe-AAdh had a weak ac-CoA reduction activity, indicating that ac-CoA reduction was the rate limiting step for ethanol formation. Furthermore, Fe-AAdh of Tne exhibited the thermostability of a hyperthermophilic enzyme with 1-h half-life at about 92 °C. In comparison, AdhB from Tet has a specific activity below 0.1 U/mg under cell growth conditions although it is highly stable, having a 1-h half-life at 85 °C or higher. AdhE has specific activities as high as 113 and 29 U/mg for the forward and reverse reactions between ac-CoA and ac-ald under simulated physiological conditions, nevertheless, it loses more than 50% activity after an incubation of 30 min at 70 °C and pH 6.5 [12].

Although having ac-CoA reduction activity in enzymology assay, Fe-AAdh did not show significant activity under imitative physiological conditions designed to approximate the enzyme roles in a cell. This could be because the imitative physiological conditions were based on the cofactor concentrations that were determined after the reducing power had been balanced by H_2 production in Tne cells. The function of fermentation pathway is mainly to dump the reducing power of NAD(P)H produced in glycolysis during anaerobic microbial growth. The reduction of ac-CoA is the first step in dumping the reducing power in the ethanol fermentation pathway, and its activity may need to be triggered by high concentrations of the reduced nucleotide cofactors. However, there is a strong Fe-hydrogenase to utilize ferredoxin and NADH synergistically for anaerobic H_2 production, so that H_2 becomes the main fermentation product of Thermotoga spp. [25]. Thus, the reducing power was balanced by Fe-hydrogenase, such that no excessive NAD(P)H to be dumped by ethanol fermentation in Tne cells when the concentrations of NAD(P)H and $NAD(P)^+$ were measured. We assume that ethanol formation can be achieved by knocking out or weakening the enzyme activities on H_2 and acetic acid formation.

Biosyhesis and metabolic engineering has been useful approach to the reconstruction of the fermentation pathways to produce desired products. For designing a pathway to be constructed, we need to find enzymes and understand the biochemical and physiological properties of the enzymes driving the target product fermentation inside microbial cells. To obtain the best results, most enzymes need to be improved by mutagenesis, truncation and/or fusion in vitro. In this study, we found CoA-dependent aldehyde dehydrogenase activity and have shown the existence of a hyperthermophilic ethanol fermentation pathway by which ac-CoA is converted to ethanol in Thermotoga spp. Although the activity of Fe-AAdh in Tne in the reduction of ac-CoA is much lower than that of AdhE in Tet, Fe-AAdh can be a basic framework for in vitro synthesis of a highly active hyperthermophilic CoA-dependent aldehyde dehydrogenase. This can be achieved by site-directed mutagenesis, motif re-assembly between Fe-AAdh and AdhE, or by directed gene evolution in large scales [26].

The regulation system and mechanism of anaerobic fermentation pathways also exist in Thermotoga [23, 27], and therefore, the systematic regulation of the enzymes involved in ethanol fermentation pathway can be an applicable parameter in the design of biosynthetic Tne. It is also known that T. maritima has a much more active phosphate acetyltransferase with a V_{max} of 260 U/mg and apparent K_m of 23 μM for ac-CoA [28], which may consume acetyl-CoA quickly, resulting in only trace amount of ethanol production when growing on glucose. Decrease in the phosphate acetyltransferase activity may be achievable through transcriptional regulation and/or enzyme engineering, further promoting a higher efficiency of ethanol fermentation at high temperatures. To prove that aldehyde ferredoxin oxidoreductase (AOR) was responsible for reducing the acetate to ac-ald, the gene encoding AOR (PF0346) was deleted in strain A. As expected, the new P. furiosus strain A/Δaor, containing Thermoanaerobacter strain X514 AdhA but lacking the host's AOR, generated only trace amounts of ethanol from maltose, similar to that of the original parent strain [10]. Moreover, the in vitro ethanol formation tests indicate very strong synergies between Fe-AAdh and other Adhs. Hyperthermophilic archaeon Pfu contains PF_0075, a gene encoding an enzyme with 94% similarity to Fe-AAdh (Table 4). The increase in ethanol production in the recombinant Pfu after a single gene was inserted to encode AdhA, a mono functional alcohol dehydrogenase, can be resulted from the synergy between AdhA and the Fe-AAdh encoded by PF_0075.

Conclusion

Hyperthermophilic Thermotoga spp. are excellent candidates for cellulosic ethanol fermentation. A hyperthermophilic Fe-AAdh was, for the first time, revealed to catalyze ac-CoA reduction to form ethanol via an acetaldehyde intermediate. Fe-AAdh and three other alcohol dehydrogenases synergically build up an ethanol fermentation pathway in Tne. The Fe-AAdh gene is highly conserved in Thermotoga spp. and in Pyrococus sp., which is probably responsible for ethanol metabolism in hyperthermophiles. The findings revealed the existence of a hyperthermophilic fermentation pathway from ac-CoA to ethanol, and offered a basic frame for in vitro synthesis of a highly active AAdh for effective ethanol fermentation pathway in hyperthermophiles, which is a key element for the approach to the consolidated processes of cellulosic ethanol production.

Materials And Methods

Bacterial strains and plasmids

Tne strain NS-E (DSM 4359) was purchased from the German Collection of Microorganisms and Cell Cultures (DSMZ). The organism was grown anaerobically in T. maritima basal medium (TBM) with 0.5% glucose at 80 °C [29]. The inhibitory effect of acetaldehyde (ac-ald) or ethanol on the growth of Tne was determined by adding various amounts of the solvent to the same medium.

Escherichia coli JM109 (Promega) was used as host for cloning and expression of genes in a pHsh vector constructed by this laboratory (Shine E Biotech,Nanjing□China). E. coli cells were routinely grown aerobically in Luria-Bertani (LB) medium at 30 °C, and 100 μg/ml ampicillin was added to the LB medium for selective cultures.

Molecular cloning and sequencing

The expression vector pHsh was linearized by inverse PCR using a pair of primers with sequences: 5´-AGCGATAGCA GTTTTTTTCAT GGGTATATCT CCTTCTTGTC-3´ upstream, and 5´-GTATCTAGAC ACCACCACCA CCACCACTAA TAA-3´ downstream. The PCR product was digested by restriction enzyme Xba I such that the linear vector had a blunt end upstream of the target gene, and a sticky end of Xba I that was ligated to the 3´-end of a target gene with a fused His-tag.

Genomic DNA was isolated from Tne cells according to the method described by Sambrook and Russell [30]. According to the annotation of the genomic sequence of Tne (GenBank accession No. CP000916.1), the genes CNT_0580, CTN_1655, and CTN_1756 are open reading frames coding for three putative iron-containing Adhs (Fe-Adh), while CTN_0257 and CTN_1548 are genes encoding a zinc-containing Adh (Zn-Adh) and an Aldh, respectively. These genes were amplified by PCR using Pyrobest DNA polymerase (Takara) with the primers listed in Table 5 and synthesized by Sangon Co. (Shanghai, China). PCR products were digested by Xba I and ligated to pHsh vector to yield expression plasmids.

Table 5
Primer sequences used in PCR amplification of genomic genes.

Primer names	Primer sequence (5′ → 3′)
CTN_0257-N	AAGGCGGTGAGGCTTCATGCAAA
-C	GGTTCTAGACTCGTTCACCATGGTAACCTT
CNT_0580-N	TTCAAAATATCATGTTATCTTCC
-C	GGTTCTAGAGTAACACCTTCTGAATATCTC
CTN_1548-N	AAAATGCTGGTTGCGGGCAGATG
-C	GGTTCTAGACTCCCTCAAATCAAAGATGAC
CTN_1655-N	GGGAACATGTGGGAGTTCTACAT
-C	GGTTCTAGACACACTCAGGGCCTCCCTGTA
CTN_1756-N	ATGGAGAATTTCGTCTTTCACAA
-C	GGTTCTAGATTTTGCGGCTATTTTCAATAT

Gene expression and enzyme purification

E. coli JM109 cells were transformed using the expression plasmids containing the Adh or Aldh genes and were grown at 30 °C to an OD_{600} of 0.6–0.8 before the cultures were transferred to a 42 °C shaking water-bath incubator for heat-shock induction of gene expression. After 6 h of cultivation along with gene expression at 42 °C, cells were harvested and transferred into an anaerobic chamber for the isolation and purification

of recombinant enzymes. E. coli cells were re-suspended in degassed 3-(N-morpholino) propanesulfonic acid buffer (MOPSb, 25 mM, pH 6.5), and disrupted by sonication, followed by heat treatment at 75 °C for 30 min.

After the cell debris and heat denatured protein were removed by centrifugation (14,000 × g, 30 min), the supernatants were mixed with the same volume of 2 × binding buffer, and loaded to the Ni-metal affinity column (Novagen) according to the manufacturer's instructions. Each recombinant enzyme bound to Ni-column was eluted, and collected into a dialysis bag, concentrated by embedding the dialysis bag in PEG 20000, and dialyzed against MOPSb with two changes. Purified enzymes were stored in MOPSb with the addition of 10% glycerol, 1 mM dithiothreitol (DTT), 0.02% (w/v) NaN_3, and 1 mM $FeCl_2$ or $ZnCl_2$ for Fe-Adhs or Zn-Adh, respectively.

Gene expression levels and the purity of recombinant proteins were examined using SDS-PAGE as described by Laemmli [31]. Protein concentration was determined by measuring the absorbance at 280 nm and calculating the concentration based on the extinction coefficient for the amino acid sequence of each enzyme.

Determination of cofactor concentrations in Tne cell fluids

Tne cells were grown to late logarithmic phase, harvested by centrifugation (10,000 × g, 10 min), and washed 3 × with saline (0.9% NaCl, w/v). Cell-free extracts were prepared by re-suspending the cells in ddH_2O, disrupting cells by sonication, and removing cell debris via centrifugation (12,000 × g, 20 min). Reduced and oxidized forms of nicotinamide adenine dinucleotide and its phosphates, NADH, NADPH, NAD^+, and $NADP^+$ were extracted from cell-free extracts by using COMINBIO Kits (Keming Co., Suzhou, China) according to manufacturer's instructions, and quantitated by high performance liquid chromatography (HPLC). An aliquot of 20 μl was analyzed using Shimadzu LC-20AD system (Shimazu, Japan) fitted with a ZORBAX Sb-aq column (250 mm × 4.6 mm) and UV/vis detector (SPD-20A). Isocratic elution conditions with a mobile phase of acetonitrile/PBST (100 mM phosphate buffer with 0.9% NaCl and 10 mM tetrabutyl ammonium bromide, pH 6.5) (9:1 v/v) were used at a flow rate of 1 ml/min, 35 °C. NAD and NADP were detected at 254 nm, NADH and NADPH were detected at 340 nm.

Enzyme activity assay

Aldh and Adh activities were measured by monitoring the changes in NAD(P)H absorbance at 340 nm. One unit of enzyme activity was defined as the amount of enzyme producing or consuming 1 μmol of NAD(P)H per min. All the activity assays were performed in triplicate, and data reported here are the mean of the three replicates. For standard enzyme activity assays, the reaction mixture consisted of 100 μl of MOPSb containing suitable substrates at concentrations: 1 mM $NAD(P)^+$ or NAD(P)H, 2 mM ac-CoA or CoASH, and 20 mM ac-ald or ethanol, at optimal pH and temperatures as indicated for each reaction (Table 1). The CoA-dependent Aldh activity was determined as described by Pei et al. [2010], and the CoA-independent Aldh activity was measured using 20 mM ac-ald as the substrate and 1 mM $NAD(P)^+$ as the cofactor, in the absence of CoASH, at 85 °C and various pH values.

For estimation of the physiological role of an enzyme, activities of recombinant Adhs were determined under conditions imitating those in the growing cells, where reactions occurred at 80 °C, pH 6.5 (MOPSb) in the presence of proportionally mixed NAD^+, $NADP^+$, NADH, and NADPH.

Determination of ethanol concentration produced from ac-CoA

The enzymatic production of ethanol from ac-CoA was measured by both gas chromatography (GC) and HPLC, and the final ethanol concentration was determined using a calibration curve prepared by linear regression plot of known concentrations of ethanol, which was processed under the same assay conditions. In vitro formation of ethanol from ac-CoA was determined in a 100 μl reaction mixture by adding Fe-AAdh (47 μg) with or without the addition of Fe-Adh1 (22 μg), Fe-Adh2 (19 μg), or Zn-Adh (43 μg). The reaction mixture contained 5 mM acetyl-CoA and 5 mM NADPH in 100 mM MOPS buffer at pH 7.0; the reaction was performed at 80 °C for 10 min followed by cooling down in an ice bath.

Aliquots of 20 μl of reaction mixture were analyzed using a Shimadzu LC-20AD system (Shimadzu, Japan) equipped with a BIO-RAD HPX-87H column (300 mm × 7.8 mm). Isocratic elution was performed with a mobile phase of 5 mM H_2SO_4 at a flow rate of 0.5 ml/min, at 50 °C. Ethanol was detected by using a refractive index detector (RID-10A). GC was performed using a Shimadzu GC-2010 system (Shimazu, Japan), and separation took place in an Rtx-1 column (30 mm × 0.25 mm) at 65–130 °C with N_2 as the carrier gas at a flow rate of 4 ml/min. The injection temperature and the FID detector temperature were 200 °C.

Abbreviations

ac-ald
acetaldehyde; ac-CoA:acetyl-coenzyme A; Adh:alcohol dehydrogenases; Aldh:aldehyde dehydrogenase; AOR:aldehyde ferredoxin oxidoreductase; CoA-Aldh:Coenzyme A dependent aldehyde dehydrogenase; DSMZ:the German Collection of Microorganisms and Cell Cultures; DTT:dithiothreitol; Fe-AAdh:iron containing bifunctional acetaldehyde/alcohol dehydrogenase; Fe-Adh1 and Fe-Adh2:iron containing alcohol dehydrogenases, number 1 and 2; GC:gas chromatography; kD:kilo Dalton; HPLC:high performance liquid chromatography; Km and Vmax:Michaelis constant and maximum reaction velocity of an enzyme; $NAD(P)^+$, NAD(P)H:oxidized or reduced type of nicotinamide adenine dinucleotide (phosphate);

NaN_3:Sodium azide; MOPSb:3-(N-morpholino) propanesulfonic acid buffer; PCR:polymerase chain reaction. OD_{600}:bacterial cell turbidity measured at 600 nm of wave length; PDC:CoA-dependent pyruvate decarboxylase; Pfu:Pyrococcus furiosus; PEG:polyethylene glycol; POR:pyruvate ferredoxin oxidoreductase; SDS-PAGE:sodium dodecyl sulfate-polyacrylamide gel electrophoresis; Tet:Thermoanaerobacter ethanolicus; Thy:Thermotoga hypogea; Tma:Thermotoga maritima; Tne:Thermotoga neapolitana; Zn-Adh:zinc containing alcohol dehydrogenases.

Declarations

Acknowledgements

The authors gratefully acknowledge the help of Professor Xun Le and Dr Dali Wang in the determination of ethanol by using gas chromatography at Nanjing Forest University.

Authors' contributions

W.S. conceived the project and designed the tests. Q.W., C.S. and H.W. performed the tests and analyzed the data. W.S., A.E.A., K.M. and J.W. wrote and revised the manuscript. All authors discussed the results and commented on the manuscript.

Funding

The financial support of National Natural Science Foundation of China (Grant no. 31770089), and Natural Science Foundation of Jiangsu Province (Youth Fund No. BK20170541).

Availability of data and materials

The datasets analysed during the current study are available from the corresponding authors on reasonable request.

Ethics approval and consent to participate

Not applicable.

Consent for publication

Not applicable.

Competing interests

The authors declare that they have no competing interests.

References

1. Shaw AJ, Podkaminer KK, Desai SG, Bardsley JS, Rogers SR, Thorne PG, et al. Metabolic engineering of a thermophilic bacterium to produce ethanol at high yield. Proc Natl Acad Sci. 2008; 105: 13769–13774.
2. Taylor MP, Eley KL, Martin S, Tuffin MI, Burton SG, Cowan DA. Thermophilic ethanologenesis: future prospects for second-generation bioethanol production. Trends Biotechnol. 2009; 27: 398–405.
3. Le Y, Shao W. Advances in and challenges for thermophilic fermentation of cellulosic ethanol. Chin J Biotechnol. 2013; 29: 274–284.
4. Wiegel J, Ljungdahl LG. The importance of thermophilic bacteria in biotechnology. Crit Rev Biotechnol. 1986; 3: 39–107.
5. Stetter K. History of discovery of the first hyperthermophiles. Extremophiles. 2006; 10: 357–362.
6. Wagner ID, Wiegel J. Diversity of thermophilic anaerobes. Ann NY Acad Sci. 2008; 1125: 1–43.
7. Desai SG, Guerinot ML, Lynd LR. Cloning of L-lactate dehydrogenase and elimination of lactic acid production via gene knockout in *Thermoanaerobacterium saccharolyticum* JW/SL-YS485. Appl Microbiol Biotechnol. 2004; 65: 600–605.
8. Yang SJ, Kataeva I, Wiegel J, Yin Y, Dam P, Xu YS, et al. Classification of '*Anaerocellum thermophilum*' strain DSM 6725 as *Caldicellulosiruptor bescii* sp. nov. Int J Syst Evol Microbiol. 2010; 60: 2011–2015.
9. Chung D, Cha M, Snyder EN, Elkins JG, Guss AM, Westpheling J. Cellulosic ethanol production via consolidated bioprocessing at 75 °C by engineered *Caldicellulosiruptor bescii*. Biotechnol Biofuels. 2015; 8: 1–13.
10. Basen M, Schut GJ, Nguyen DM, Lipscomb GL, Benn RA, Prybol CJ, et al. Single gene insertion drives bioalcohol production by a thermophilic archaeon. Natl Acad Sci USA, 2014; 111: 17618–17623.

11. Bryant F, Wiegel J, Ljungdahl LG. Purification and properties of primary and secondary alcohol dehydrogenases form *Thermoanaerobacter ethanolicus*. Appl Environ Microbiol. 1988; 54: 460–465.
12. Pei J, Zhou Q, Jiang Y, Le Y, Li H, Peng H., et al. *Thermoanaerobacter* spp. control ethanol pathway via transcriptional regulation and versatility of key enzymes. Metab Eng. 2010; 12: 420–428.
13. Perozich J, Nicholas H, Wang BC, Lindahl R, Hempel J. Relationships within the aldehyde dehydrogenase extended family. Protein Sci. 1999; 8: 137–146.
14. Jannasch HW, Huber R, Belkin S, Stetter KO. *Thermotoga neapolitana* sp. nov. of the extremely thermophilic, eubacterial genus *Thermotoga*. Arch Microbiol. 1988; 150: 103–104.
15. Vasconcelos I, Girbal L, Soucaille P. Regulation of carbon and electron flow in *Clostridium acetobutylicum* grown in chemostat culture at neutral pH on mixtures of glucose and glycerol. J Bacteriol. 1994; 176: 1443–1450.
16. Ying X, Wang Y, Badiei H, Karanassios V, Ma K. Purification and characterization of an iron-containing alcohol dehydrogenase in extremely thermophilic bacterium *Thermotoga hypogea*. Arch Microbiol. 2007; 187: 499 – 510.
17. Notredame C, Higgins D, Heringa J, T-Coffee: A novel method for multiple sequence alignments. J Mol Biol. 2000; 302: 205–217.
18. Robert X, Gouet P. Deciphering key features in protein structures with the new ENDscript server. Nucleic Acids Res. 2014; 42: W320–W324.
19. Eram MS, Wong A, Oduaran E, Ma K. Molecular and biochemical characterization of bifunctional pyruvate decarboxylases and pyruvate ferredoxin oxidoreductase from *Thermotoga maritima* and *Thermotoga hypogea*. J Biochem. 2015; 158: 459–466.
20. Eram MS, Ma K. Pyruvate decarboxylase activity of the acetohydroxyacid synthase of Thermotogamaritima. Biochem. Biophysics Rep. 2016; 7: 394–399.
21. Burdette D, Zeikus JG. Purification of acetaldehyde dehydrogenase and alcohol dehydrogenases from *Thermoanaerobacter ethanolicus* 39E and characterization of the secondary-alcohol dehydrogenase (2°ADH) as a bifunctional alcohol dehydrogenase-acetyl-CoA reductive thioesterase. Biochem J. 1994; 302: 163–170.
22. Peng H, Wu G, Shao W. The aldehyde/alcohol dehydrogenase (AdhE) in relation to the ethanol formation in *Thermoanaerobacter ethanolicus* JW200. Anaerobe. 2008; 14: 125–127.
23. Pei J, Zhou Q, Jing Q, Li L, Dai C, Li H, et al. The mechanism for regulating ethanol fermentation by Redox levels in *Thermoanaerobacter ethanolicus*. Metab Eng. 2011; 13: 186–193 (2011).
24. Pineda E, Encalada R, Rodríguez-Zavala JS, Olivos-García A, Moreno-Sánchez R, Saavedra E. Pyruvate:ferredoxin oxidoreductase and bifunctional aldehyde-alcohol dehydrogenase are essential for energy metabolism under oxidative stress in *Entamoeba histolytica*. FEBS J. 2010; 277: 3382–3395.
25. Schut GJ, AdamsMWW. The iron-hydrogenase of *Thermotoga maritima* utilizes ferredoxin and NADH synergistically: a new perspective on anaerobic hydrogen production. J Bacteriol. 2009; 191: 4451–4457.
26. Shao W, Ma K, Le Y, Wan H, Sha C. "Development and use of a novel random mutagenesis method: *In situ* error-prone PCR (*is*-epPCR)", in In Vitro Mutagenesis: Methods and Protocols, A. Reeves ed., Methods Mol Biol. 2016; 1498: 497–506.
27. Ravcheev DA, Li X, Latif H, Zengler K, Leyn SA, Korostelev YD, Kazakov AE, Novichkov PS, Osterman AL, Rodionov DA. Transcriptional regulation of central carbon and energy metabolism in bacteria by redox-responsive repressor Rex. J Bacteriol. 2012; 194: 1145–1157.
28. Schonheit P. Phosphate acetyltransferase and acetate kinase from *Thermotoga maritima*. Methods Enzymol. 2001; 331: 168–176.
29. Jiang Y, Zhou Q, Wu K, Li X, Shao W. A highly efficient method for liquid and solid cultivation of the anaerobic hyperthermophilic eubacterium *Thermotoga maritima*. FEMS Microbiol. Lett. 2006; 259: 254–259. `
30. Sambrook J, Russell DW. Molecular Cloning: A laboratory manual. Cold Spring Harbor Laboratory Press, New York; 2001.
31. Laemmli UK. Cleavage of structural proteins during assembly of the head of bacteriophage T4. Nature. 1970; 227: 680–685.

Figures

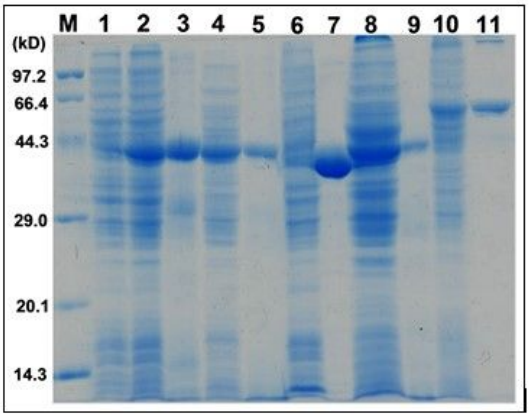

Figure 1

SDS-PAGE analysis of gene expression and enzyme purification. Lanes: M, protein markers with molecular masses as indicated; 1, Escherichia coli cell protein; 2 - 11, gene expression in E. coli and isolated gene products of gene CTN_0257 (2, 3), CNT_0580 (4, 5), CTN_1655 (6, 7), CTN_1756 (8, 9), and CTN_1548 (10, 11

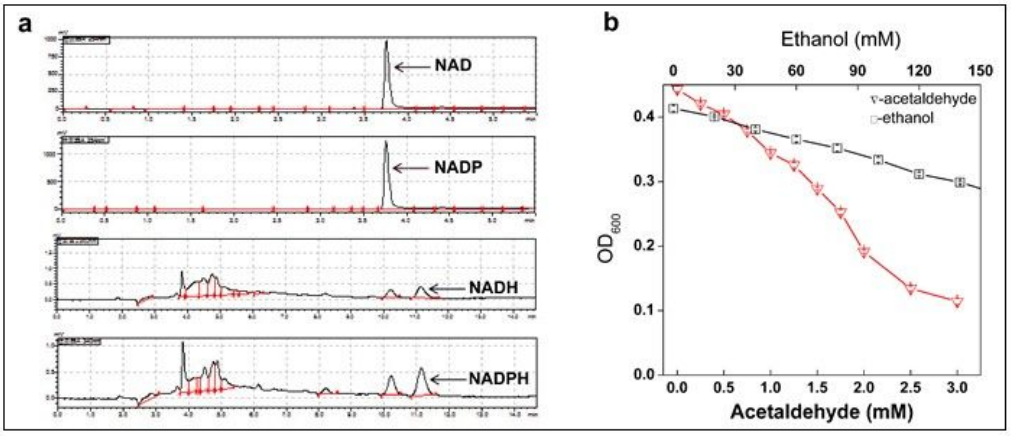

Figure 2

Composition of nucleotide cofactors in Thermotoga neapolitana (Tne) cells, and the effects of acetaldehyde and ethanol on Tne cell growth. a HPLC profiles of NAD+, NADH, NADP+, and NADPH from Tne cells. b The growth curves of Tne at different concentrations of acetaldehyde and ethanol.

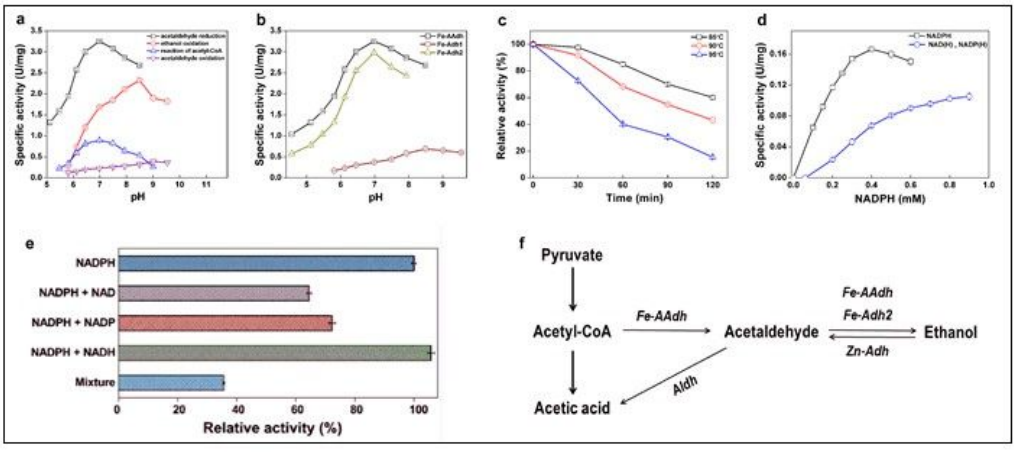

Figure 3

Properties of the bifunctional aldehyde/alcohol dehydrogenase (AAdh) and alcohol dehydrogenases of Thermotoga neapolinata. a Specific activities Fe-AAdh on the reactions in ethanol formation and consumption. b The effects of pH on the specific activities of Fe-AAdh, Fe-Adh1 and Fe-Adh2. The buffer composition for these assays was 25 mM each of phthalate, MOPS, Tris, and glycine with pH values calibrated at 80 °C. c Thermostability of Fe-AAdh. d Substrate saturation curves for NADPH in the absence or presence of NADH, NAD+, and NADP+ mixture (0 .28, 1.8, and 0.18 mM, respectively). e Effects of NADH, NAD+, NADP+, or their mixture on Fe-AAdh activity with 0.4 mM NADPH and 2 mM actyl-CoA as substrates. f The ethanol metabolic pathway identified by the activities of the enzymes determined at 80 °C, pH 6.5 with the substrate(s) needed for each step. Cofacter(s): Fe-AAdh, NADPH; Aldh, NADP+; all other enzymes, a cofactor mixture containing 1.8, 0 .28, 0.18 and 0.06 mM of NAD+, NADH, NADP+ and NADPH.

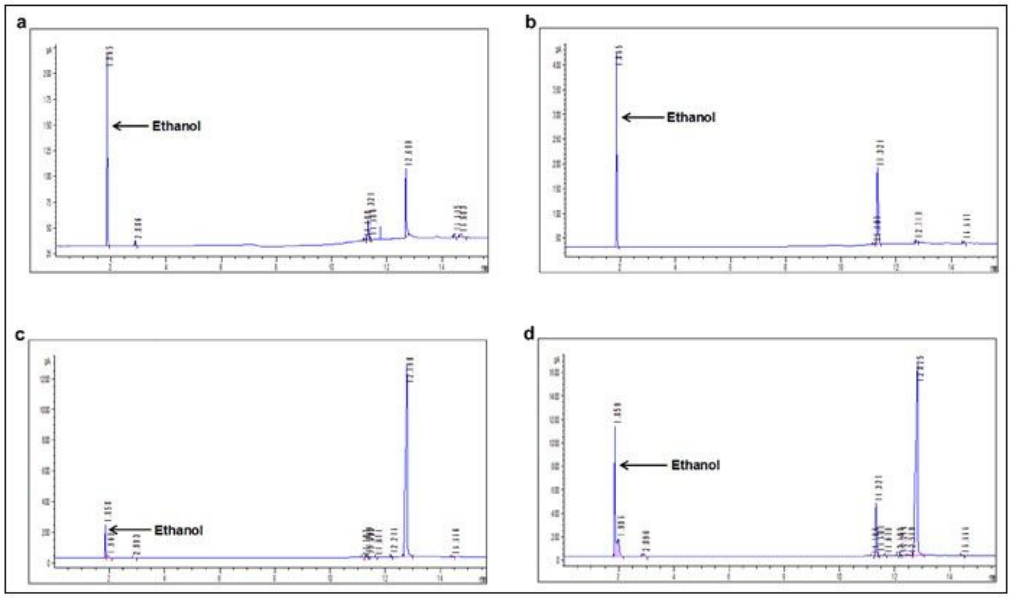

Figure 4

GC chromatograms of in vitro ethanol formation from ac-CoA. Ethanol formation catalyzed by Fe-AAdh (a), or by combined enzymes of Fe-AAdh/Zn-Adh (b), Fe-AAdh/ Fe-Adh1 (c), and Fe-AAdh/Fe-Adh2 (d). Reactions were performed at 80 °C, pH 7.0 for 10 min with 5 mM ac-CoA and 5 mM NADPH as substrates.

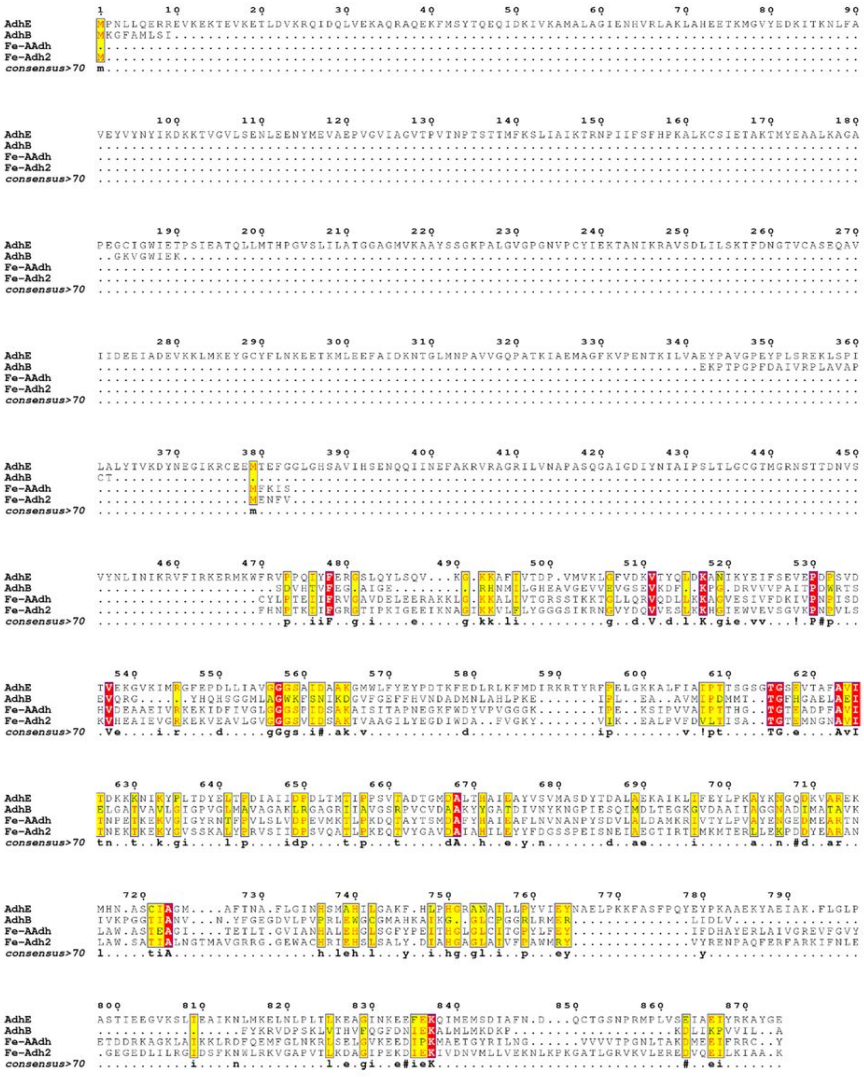

Figure 5

The alignment of the amino acid sequences of bifunctional aldehyde/alcohol dehydrogenases in comparison with Fe-Adh2, a mono functional alcohol dehydrogenase. The domain from residue 30 to 412 of AdhE is related to the aldehyde dehydrogenase family (ALDH-SF superfamily), the domain from residue 551 to 854 belongs to Fe-alcohol dehydrogenase family (PF00465).

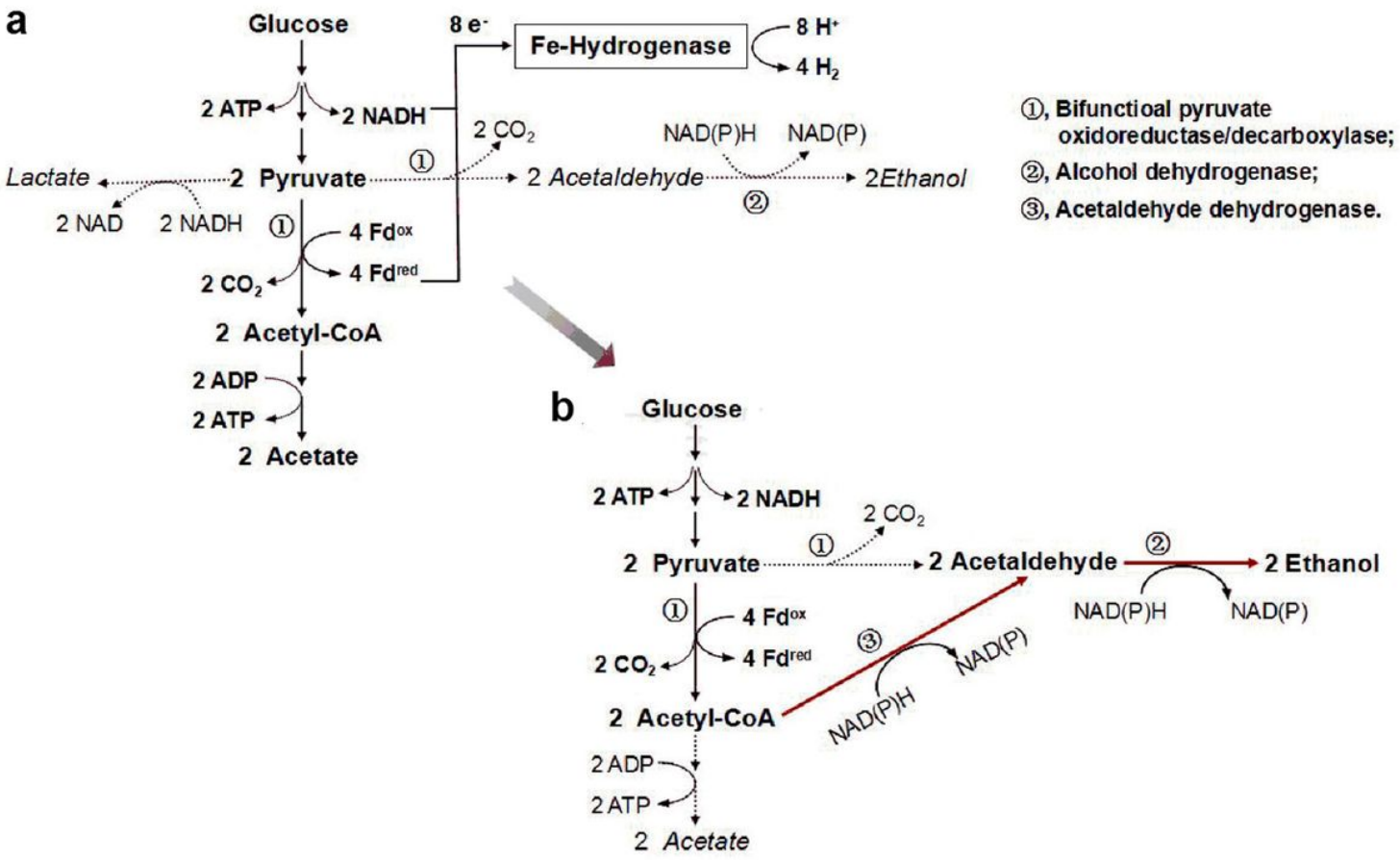

Figure 6

Schematics of the fermentation pathways of Thermotoga spp. a The original pathways in the wide-type strains. b The suggested engineered pathways to be constructed by metabolic engineering. The names in bold font are the main products or intermediates in the fermentation process; those in italic font are weak products; solid and dashed arrows indicate the strong and weak reactions, respectively.